Langmuir

Article

pubs.acs.org/Langmuir

Excited-State Dynamics of Charged Dyes at Alkane/Water Interfaces in the Presence of Salts and Ionic Surfactants

Marina Fedoseeva, Piotr Fita,† and Eric Vauthey*

Department of Physical Chemistry, University of Geneva, 30 Quai Ernest-Ansermet, Geneva, Switzerland

Supporting Information

ABSTRACT: The excited-state dynamics of the cationic dye malachite green (MG) and of the dianionic dye eosin B at the dodecane/water interface has been investigated using femtosecond time-resolved surface second harmonic generation (TR-SSHG). By using different probe wavelengths, the contributions of monomeric and aggregated MG to the signal could be spectroscopically distinguished. The effect of the addition of a small amount of surfactants was found to strongly depend on the relative charges of surfactant and dye. For surfactant/dye pairs with opposite charges, the TR-SSHG signal is dominated by the contribution from aggregates, whereas for pairs with the same charges, the signal intensity becomes vanishingly small. These effects are explained in terms of electrostatic interactions between surfactants and dyes that favor either attraction of the dye toward the interface or its repulsion toward the bulk. As a very similar behavior is observed with MG upon addition of NaSCN, we conclude that, in this case, this effect reflects the affinity of SCN^- for the interface. On the other hand, the guanidinium cation was found to have a different effect than that of a positively charged surfactant on the SSHG signal of MG, indicating this cation does not accumulate in the interfacial region.

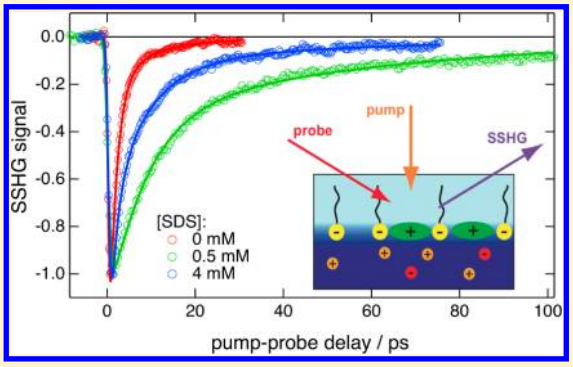

INTRODUCTION

Because of their crucial role in life and environmental sciences, liquid interfaces have been intensively studied over the past decades.[1−3] Despite the fact that interfaces segregate two immiscible liquid phases, they still act as a channel for the transfer of mass and energy between these phases. As a consequence, a comprehensive knowledge of their properties is of paramount importance for our understanding of interfacial phenomena as well as for many applications such as, for example, the design of new drugs[2] or energy conversion.[4] The key feature that distinguishes the interfaces from the surrounding bulk environments is the anisotropy of forces, which affects the orientation of the molecules, leading to properties that differ from those of the two constituting isotropic phases. However, direct insight into these properties is experimentally challenging, since the number of molecules dissolved in the bulk phases is higher by many orders of magnitude than the number of molecules adsorbed at the ∼1 nm-thick interfacial layer.[5] As a consequence, when performing conventional spectroscopy, the contribution from the interface to the signal is totally buried in that from the bulk. One of the most powerful approaches to circumvent this problem is to perform surface second harmonic generation (SSHG)[6−8] or surface sum frequency generation (SSFG)[9,10] measurements to probe the second-order nonlinear optical susceptibility, $\vec{\chi}^{(2)}$, that vanishes in isotropic media, at least within electric dipole approximation, and is thus only nonzero at interfaces.[11] As the SSH(F)G signal intensity is enhanced when the probe frequency coincides with one- or two-photon transitions, spectroscopic information on dye molecules adsorbed at the interfaces can be obtained,[6] provided these dyes have a nonzero second-order hyperpolarisability and are partially oriented.

The effect of ions on the properties of interfacial water has for many years been a major concern in chemistry as well as in biology.[12−16] Some ions, such as thiocyanate (SCN^-) or guanidinium (GuH^+), are known to affect surface tension, to increase the solubility of proteins, and to favor their denaturation, whereas others, like SO_4^{2-} and Ca^{2+}, have opposite or little effect.[17] These ions are located at the opposite sides of the Hofmeister series that sort the ions according to their salting-in or salting-out properties.[14,18−20] Therefore, these ion properties should be somehow related to their affinity for interfaces. However, the interfacial concentration of ions is not an easily accessible quantity for the reasons discussed above and, therefore, most information has been obtained from second-order nonlinear optical spectroscopy,[21−33] as well as computational chemistry.[34−36]

SSFG investigations by the Richmond and the Allen groups on the influence of salts on the structure of the air/water interface pointed to a negligible effect of NaF and NaCl but resulted in somewhat different conclusions with NaBr and NaI.[22,23] Subsequent measurements of the surface concen-

Received: June 11, 2013
Revised: September 24, 2013
Published: November 18, 2013

tration of azide ions, determined by SSHG experiments in resonance with a charge-transfer-to-solvent transition, revealed an enhanced surface concentration of anions.[24] The validity of this approach to determine surface concentration was confirmed later on using charged surfactants.[25] With the use of the same SSHG technique, enhanced concentration of SCN^- was found at the dodecanol/water interface.[29] Interfacial ions have also been directly detected by monitoring ion stretch vibrations using SSFG.[30−32] An advantage of this approach is that the ions can be precisely identified from their spectroscopic signature. On the other hand, comparison of the affinity of different ions for the interface is not straightforward, as their second-order hyperpolarisability is not the same. Moreover, in order to benefit from the resonance enhancement of the signal, probe wavelengths specific to each ion have to be used. Therefore, the possibility of comparing the relative affinity of ions for the interface by probing the very same parameter would be extremely useful.

We have recently reported on the investigation of the excited-state dynamics of the cationic dye, malachite green (MG, Chart 1), at alkane/water interfaces in the presence of various concentrations of sodium salts, using time-resolved (TR) SSHG.[20] Without salt, the SSHG intensity was found to decrease upon $S_1 \leftarrow S_0$ excitation and to recover biexponentially its original value with time constants of ∼2 and ∼20 ps. As the relative amplitude of the slow component increased with increasing MG concentration, the fast and slow components were assigned to the ground-state recovery of MG monomers and MG aggregates, respectively.[37] Addition of salt to the aqueous phase also resulted in an increase of the amplitude of the slow component by an amount that depended on the nature of the anion, the effect increasing in the order $SO_4^{2-} < Cl^- \sim < Br^- \ll SCN^-$. As this is similar to the Hofmeister series for increasing salting-in property of anions, this result was explained by the different affinity of the anions for the interface and by the electrostatic interactions between the interfacial anions and the cationic MG molecules, that favor their adsorption at the interface and, hence, their aggregation.

Chart 1. Malachite Green Cation (MG) and Eosin B Dianion (EB)

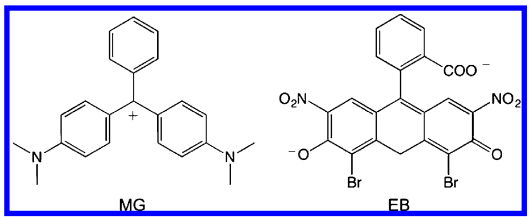

We report here on a comparison of the effect of the addition of salts and charged surfactants on the excited-state dynamics of MG at the dodecane/water interface. By definition, surfactants have a strong affinity for interfaces, with their charged head confined to the upper part of the aqueous surface and their long hydrophobic alkyl chains lying in the lipophilic phase.[38,39] This leads to a charging of the interface, similar to that which should occur for ions, like SCN^-, that are thought to have a preferential affinity for interfaces. Therefore, if the enhanced aggregation of MG upon addition of salting-in anions indeed arises from electrostatic interaction, the same effect should be observed with a negatively charged surfactant. The present investigation reveals that this is actually the case. Further results obtained with a positively charged surfactant, with guanidinium chloride and with the dianionic dye eosin B (EB, Chart 1) will also be presented. In our previous study,[20] the contribution of MG monomers and MG aggregates was only inferred from their different ground-state recovery dynamics. Here, both species are also spectrally distinguished using a TR-SSHG setup with a tunable probe wavelength.

EXPERIMENTAL SECTION

Samples. Malachite green (MG) oxalate and eosin B (EB) disodium were purchased from Fluka and Sigma-Aldrich, respectively. The salts, sodium thiocyanate (NaSCN) and guanidinium chloride (GuHCl), were from Fluka and AppliChem, respectively, whereas the surfactants, sodium dodecyl sulfate (SDS) and cetyltrimethylammonium bromide (CTAB), were from AppliChem and Acros Organics, respectively. The aqueous solutions were prepared by dissolving the dyes and salts or surfactants at concentrations specified further for each experiment in deionized water and were poured into a 4 × 4 × 4 cm^3 optical glass cell. In all measurements, the pH of the aqueous solutions remained between 5 and 7, a range where MG and EB are in the monocationic and dianionic form, respectively.

In all experiments, the upper organic phase was dodecane (Acros Organics, 99%). All compounds were used without further purification.

Stationary SSHG Measurements. Measurements of the stationary SSHG intensity between 385 and 520 nm were performed with a setup based on a Ti:Sapphire oscillator (MaiTai, Spectra-Physics), generating ∼100 fs pulses at 82 MHz, tunable between 770 and 1040 nm. About 300 mW of the laser output beam was focused with a 500 mm lens onto the interface with an angle of incidence of about 70°, where it underwent total internal reflection. To eliminate unwanted SSHG signal originating from the surfaces of the optical components, a long-pass filter was located just in front of the sample cell. The SSHG signal was collected by a 100 mm lens, cleaned out from the fundamental probe light with a short-pass filter, and focused onto the entrance slit of a 0.25 m monochromator (Cornerstone 260, Oriel) with a 60 mm lens, before being detected with a photomultiplier tube operating in photon counting mode (R6353P, Hamamatsu). The digitized output of the counting electronics was read by a computer that also controlled the tuning of the laser wavelength. The SSHG intensity was corrected for the wavelength dependence of the output power and the spectral response of the optics and detection. The wavelength dependence of the pulse duration was not taken into account.

Time-Resolved Surface Second Harmonic Generation (TR-SSHG). Two different TR-SSHG setups have been used. In the first one, described in detail elsewhere,[40,41] probing was performed at 800 nm only. Briefly, the pump pulses (∼50 fs) were generated by a noncollinear optical parametric amplifier (OPA, Clark-MXR) pumped by a fraction of the output of a Ti:sapphire amplified system (Spitfire, Spectra-Physics) and were circularly polarized. They were focused on the interface from the top using a combination of spherical and cylindrical lenses. Probing was achieved at 800 nm with another fraction of the output of the Ti:sapphire amplified system (∼100 nJ, ∼100 fs, 1 kHz) with a geometry similar to that used for the stationary SSHG measurements. Collection and detection of the SSHG signal at 400 nm were also similar, except that the detector was a multipixel photon counter avalanche photodiode (S-10362-11-050U, Hamamatsu). Its output signal was processed with a boxcar-gated integrator and averager module before being digitized and stored in a computer.

The second TR-SSHG setup allowed the probe wavelength to be tuned. The pump pulses (3−4 μJ at the interface, ∼80 fs) were generated with a two-stage noncollinear OPA (TOPAS White, Light Conversion), whereas the probe pulses (50−200 nJ at the interface, ∼100 fs) were produced with a collinear OPA (TOPAS C, Light Conversion) allowing full tunability in the UV, Vis, and mid-IR ranges. Both TOPAS were pumped by 1 mJ and 100 fs pulses at 800 nm produced by a 1 kHz Ti:sapphire-amplified system (Solstice, Spectra-Physics).

dx.doi.org/10.1021/la402191p | Langmuir 2013, 29, 14865−14872

The beam geometry and SSHG signal collection were similar as in the above-described setups. The signal was focused onto the entrance slit of a Czerny–Turner spectrograph (Shamrock 163, Andor), equipped with a multipixel-cooled CCD camera (Newton 920, Andor). The illuminated pixels were vertically binned, summed over the wavelength range of interest, and the resulting value transferred to a computer.

In all experiments and all setups, the pump pulses were circularly polarized, the probe pulses were s-polarized, and the p-polarized component of the SSHG signal was detected.

The nonresonant contribution to the SSHG signal measured without dye in the aqueous phase was found to be vanishingly small. Therefore, with dye present in the aqueous phase, the SSHG signal has a purely resonant character of dipolar origin,[42] and its intensity depends on the square modulus of the relevant elements of the second-order nonlinear optical susceptibility tensor, $\vec{\vec{\chi}}^{(2)}$, hence on the square of the number of dye molecules contributing to the signal.[41] Analysis of the TR-SSHG profiles was performed on a processed signal, $S(t)$, obtained by first taking the square root of the measured SSHG intensity and, second, normalizing the resulting values so that S is equal to zero at negative pump–probe delays and is equal to either 1 or −1 at its maximum photoinduced change, depending on whether the SSHG signal increases or decreases upon excitation, respectively. The so-obtained signal intensity, $S(t)$, is proportional to the photoinduced population changes. Analysis of these time profiles was performed by nonlinear least-squares fitting using the Levenberg–Marquardt algorithm, as implemented in IgorPro (version 6.3, Wavemetrics Inc.). The fitting function was the analytical expression for the convolution of a mono- or multiexponential function accounting for the population dynamics with a Gaussian function accounting for the instrument response, as described in ref 43. The width of the instrument response function, estimated from the initial photoinduced change of the SSHG signal that was assumed to be prompt, was about 750 fs for both setups. This relatively large value mostly arises from the pump and probe beams geometry.

RESULTS AND DISCUSSION

Interfacial Excited-State Dynamics of MG. Figure 1 shows the electronic absorption spectrum of MG in water

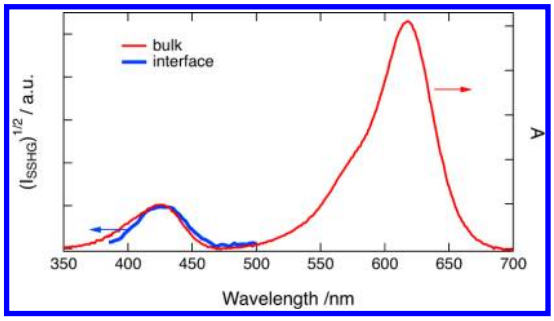

Figure 1. Stationary SSHG spectrum of MG at the dodecane/water interface and electronic absorption spectrum of MG in water.

together with the SSHG spectrum measured with MG at the dodecane/water interface. The band culminating at 618 nm corresponds to the $S_1 \leftarrow S_0$ transition, whereas that at 425 is due to the $S_2 \leftarrow S_0$ transition. The square-root of the SSHG signal intensity measured upon probing between 760 and 1000 nm matches the linear absorption spectrum between 380 and 500 nm, pointing to a signal enhancement via a two-photon resonance. A similar result has recently been obtained at the air/water interface by Tahara and co-workers using broadband electronic SSFG.[44]

Previous TR-SSHG investigations of MG have been carried out using single wavelength probing at either 800 or 625 nm (i.e., either in two-photon resonance with the $S_2 \leftarrow S_0$ transition or in one-photon resonance with the $S_1 \leftarrow S_0$ transition).[20,37,40,45] In both cases, excitation was performed in the $S_1 \leftarrow S_0$ band, and the SSHG intensity was found to decrease upon excitation and to return biexponentially to its initial value on a few picoseconds and a few tens of picoseconds timescales, the amplitude of the faster component being typically 10 times as large as that of the slower one. The fast component, which has been found to slow down upon addition of glycerol in the aqueous phase, was ascribed to the ground-state recovery of MG upon nonradiative relaxation from the S_1 state,[44,45] the viscosity dependence being due to the effect of solvent friction on the large amplitude motion that is required to reach the S_1/S_0 conical intersection. The slow component, observed at both air/water and alkane/water interfaces, was originally ascribed to the relaxation from the distorted MG ground state.[40,44] However, the increase of its amplitude with increasing MG concentration found subsequently at alkane/water interfaces indicated that, at these interfaces at least, this slow component is due to the ground-state recovery of MG aggregates.[37] Figure 2 shows TR-SSHG profiles, $S(t)$, obtained

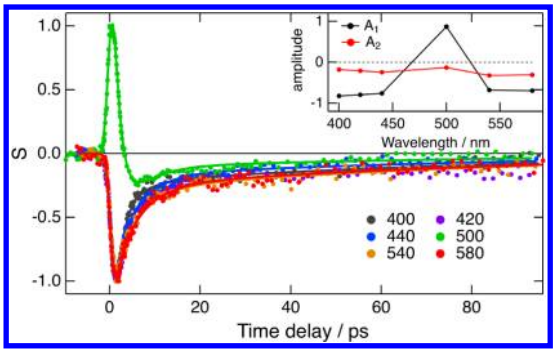

Figure 2. TR-SSHG profiles measured at different wavelengths with MG (1.5×10^{-4} M) at the dodecane/water interface. Inset: amplitudes of the fast (A_1, 1.3 ps) and slow components (A_2, 23 ps) obtained from global biexponential analysis.

by probing the interface between 800 and 1160 nm upon 618 nm excitation. Except for that measured at 500 nm (i.e., upon probing at 1000 nm), these profiles are almost identical and exhibit a prompt decrease at time zero followed by a biphasic recovery of the intensity, as previously observed upon 625 and 800 nm probing. This result is also in agreement with the TR-SSFG signal measured between 360 and 470 nm with MG at the air/water interface by Tahara and co-workers.[44]

By contrast, the TR-SSHG profile at 500 nm exhibits first a prompt rise at time zero, indicative of an increase of the SSHG intensity upon excitation, followed by a fast decay to a negative value and by a subsequent rise to zero. All these profiles could be well-reproduced by the convolution of a Gaussian function, accounting for the instrument response with the sum of two exponential functions with time constants of 1.3 ± 0.2 and 25 ± 2 ps, and the relative amplitudes shown in the inset of Figure 2. Figure 1 indicates that the stationary SSHG intensity at 500 nm is very weak because of the absence of a resonance enhancement. On the other hand, previous transient absorption measurements in bulk solutions revealed the presence of a $S_n \leftarrow S_1$ absorption band between 450 and 550 nm.[37,40] As a consequence, the positive component of the TR-SSHG signal at 500 nm is ascribed to a resonance with the $S_n \leftarrow S_1$ transition, and its temporal evolution reflects that of the S_1

dx.doi.org/10.1021/la402191p | Langmuir 2013, 29, 14865–14872

state population of MG. At the other wavelengths, the resonant enhancement is dominated by the two-photon $S_1 \leftarrow S_0$ and $S_2 \leftarrow S_0$ transitions, and the fast component of the TR-SSHG signal reflects the ground-state recovery of MG.

Figure 3 shows that the relative amplitude of the positive signal component at 500 nm strongly decreases upon increasing

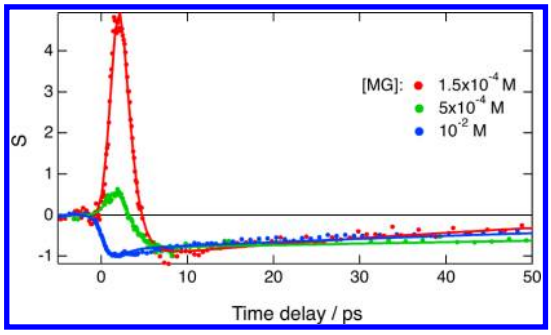

Figure 3. TR-SSHG profiles measured at 500 nm with different bulk concentrations of MG at the dodecane/water interface (for better comparison, the profile at low concentration was normalized at −1).

MG concentration and totally vanishes at 10^{-2} M. This effect fully supports the assignment of this short-lived positive feature to the MG excited state. It further confirms that the slow component is due to MG aggregates. Aggregation of MG in aqueous solution can be triggered upon addition of a salt, like NaCl, and leads to an intensity decrease at the maximum of the $S_1 \leftarrow S_0$ band and to the rise of a shoulder on both sides.[40] On the other hand, only a slight red shift of the $S_2 \leftarrow S_0$ band is observed. Additionally, the intensity of the $S_n \leftarrow S_1$ transient absorption band in the 450−500 nm region was found to decrease substantially upon addition of NaCl, indicating that the excited-state absorption of MG aggregates in this region is smaller than that of the monomer.[40] This is in excellent agreement with the wavelength dependence of the slow component of the TR-SSHG profiles, which is always associated with a negative amplitude. Therefore, this slow component reflects the ground-state recovery of MG aggregates.

Addition of Salts. Among the sodium salts previously investigated, NaSCN was found to lead to the most pronounced changes in the excited-state dynamics of MG.[20] Addition of NaSCN to the aqueous phase is accompanied by a continuous increase of the stationary SSHG intensity going from a factor of about two at only 5 mM to a factor of more than ten at 100 mM (Figure S1 of the Supporting Information). The effect of NaSCN on the TR-SSHG profiles is the same at all wavelengths except at 500 nm. As illustrated in Figure 4, the recovery of the TR-SSHG signal is strongly slowed down in the presence of NaSCN. Biexponential analysis of these profiles reveals that this slowing down of the dynamics is in fact due to an increase of the amplitude of the slow component, associated with the ground-state recovery of aggregates, relative to that of the fast component.

At 500 nm, addition of NaSCN has the same influence on the TR-SSHG profile as the increase of the concentration of MG (i.e., the amplitude of the positive component decreases with increasing salt concentration and totally vanishes at 50 mM) (Figure S2 of the Supporting Information). However, the time constants associated with slow and fast components are not significantly affected. As a consequence, this effect can be

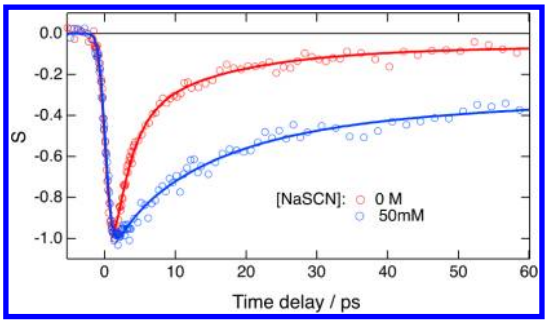

Figure 4. TR-SSHG profiles measured at 420 nm with MG (1.5×10^{-4} M) at the dodecane/water interface with and without NaSCN.

ascribed to an increased population of MG aggregates and to a parallel decrease of MG monomers at the interface. This effect has previously been proposed to be due to the affinity of SCN^- for the interface.[20] This leads to an electrostatic attraction of the positively charged MG toward the interface and to the formation of aggregates.

The structure of the aggregate is not known, but seems to be the same in pure water at high MG concentrations and upon addition of salt. Indeed, the spectral and temporal dependences of the TR-SSHG signal are very similar. Moreover, the same time constant associated with the ground-state recovery of the aggregate was found with several different sodium salts,[20] indicating that the nature of the MG aggregate measured at the interface does not depend on the anion.

There is also a Hofmeister series for cations, according to their salting-in properties,[17] which should also reflect their interfacial affinity. It is generally assumed that small non-polarizable hard cations, such as Na^+ and K^+, are repelled from the surface,[12,17,34] even though there has been no systematic study on this matter. On the other hand, cations located at the other side of the Hofmeister series, such as guadinium cation, GuH^+, are expected to exhibit the highest interfacial affinity.[17] Guanidinium chloride is also known to be one of the most effective protein denaturants.[46]

Addition of GuHCl to the aqueous phase leads to an increase of the stationary SSHG signal intensity by a factor of less than 2, but does not affect the TR-SSHG profile (Figure 5 and Figure S3 of the Supporting Information). These two results seem contradictory as, on one hand, the first points to an increase of the interfacial concentration of MG and, on the other hand, the second indicates that aggregation is not enhanced. If GuH^+ were accumulating at the interface, a

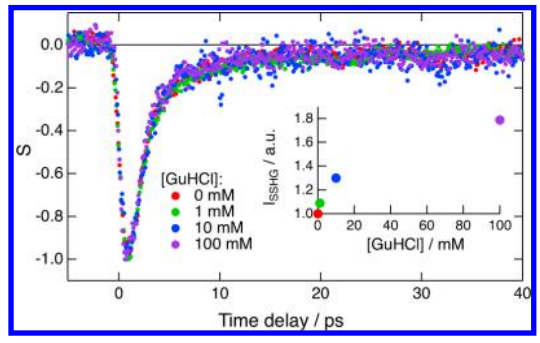

Figure 5. TR-SSHG signal profiles measured at 400 nm with MG (1.5×10^{-4} M) and various concentrations of GuHCl at the dodecane/water interface. Inset: dependence of the relative stationary SSHG intensity at 430 nm on the GuHCl concentration.

dx.doi.org/10.1021/la402191p | Langmuir 2013, 29, 14865−14872

depletion of the interfacial MG concentration would be expected because of the electrostatic repulsion between both cationic species. Recent molecular dynamics simulations of GuH^+ at the air/water interface indicate that, despite being on the salting-in side of the Hofmeister series of cations, GuH^+ is rather depleted from the interfacial region.[47] This finding also agrees with surface tension measurements.[17] On the other hand, an anisotropic orientation of GuH^+, with the molecular plane parallel to the interface, was found in these simulations.[47] Such a low interfacial affinity of GuH^+ can explain the negligible effect of GuHCl on the TR-SSHG profiles. However, it cannot account for the observed increase of stationary SSHG signal. It should be noted that this increase of intensity is much smaller than that found with SCN^-.[40] Addition of NaCl has been found to also favor adsorption of MG at the interface but to a much smaller extent than NaSCN.[20,40] Therefore, the increase of the SSHG signal could be due to the interfacial Cl^- population. However, with this rather modest salt concentration, the effect is too small to significantly affect the population of aggregates. Additionally, the orientational anisotropy of GuH^+ found from molecular dynamics simulations could increase the orientational anisotropy of the MG dyes at the interfaces and could therefore lead to an enhancement of the SSHG intensity.

Addition of Ionic Surfactants. The above-described effects observed upon addition of salts can be interpreted in terms of the interfacial affinity of the ions. In other words, the increased aggregation of MG with NaSCN originates from a negative charging of the interface, whereas the increased SSHG signal with GuHCl rather indicates that the interface is not positively charged.

Similar interfacial experiments have been carried out with ionic surfactants to establish the effect of the charge of the interface on the SSHG properties of MG. Figure 6 shows TR-SSHG profiles as well as the stationary SSHG intensity with different concentrations of the anionic surfactant SDS.

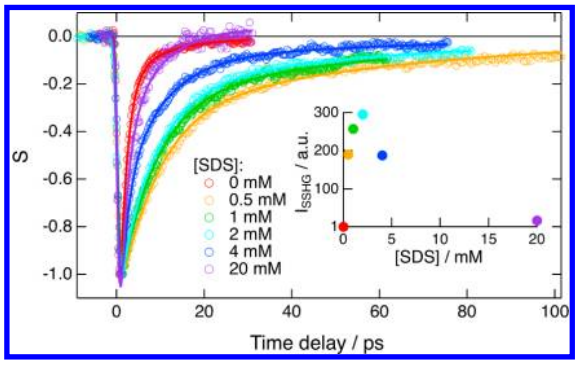

Figure 6. TR-SSHG profiles measured at 400 nm with MG (10^{-5} M) and various concentrations of SDS at the dodecane/water interface. Inset: dependence of the stationary SSHG intensity at the band maximum on the SDS concentration.

Small concentrations of SDS lead to a strong increase of the SSHG intensity, the maximum of which is reached at approximately 2 mM. Further addition of SDS up to a concentration exceeding the critical micellar concentration (CMC), which is around 8 mM,[48] causes a decrease of the SSHG intensity down to about the same value as that without surfactant. The TR-SSHG profiles are also affected by the presence of SDS. A strong slowing down of the signal recovery dynamics at 400 nm is observed with a small amount of SDS. At 500 nm, the positive feature due to MG monomer in the S_1 state has totally vanished at 0.1 mM SDS (Figure S4 of the Supporting Information). The TR-SSHG profiles remain essentially the same up to about 2 mM SDS. At higher SDS concentrations, the signal recovery dynamics become faster and, at 20 mM SDS, it is almost as fast as without the surfactant. Multiexponential global analysis of the TR-SSHG profiles at different SDS concentrations required not less than three exponential functions with 1.7 ± 0.2, 10 ± 1 and 62 ± 4 ps. The relative amplitude of the fast component amounts to 0.94 in the absence of SDS, drops to essentially zero at 0.5 and 1 mM SDS, and increases again up to 0.7 at the highest concentration. The amplitude of the two slower components shows the opposite trend with that of the 10 ps component remaining larger than that of the 62 ps component. Whereas the fast component can be assigned to MG monomers, the two slowest are ascribed to MG aggregates. The fact that three exponentials were required here is most probably due to the superior signal-to-noise ratio of the profiles measured with small SDS concentrations and to the high relative amplitude of the slow components. In the other cases, the amplitude of the slow recovery is too small to make three-exponential analysis relevant.

The initial rise of the SSHG intensity with SDS concentration can be attributed to an increase of the number of MG molecules contributing to the signal. It can have two origins: (1) an enhanced adsorption of MG at the interface favored by electrostatic interactions between the negatively charged interface and the cationic dyes and (2) the existence of an orientational anisotropy of the MG molecules not only at the interface but also deeper in the aqueous phase because of the static electric field, $\vec{\Phi}(0)$, associated with the charged surfactants at the interface. In such case, the SSHG signal originates from both the second- and third-order nonlinear polarizations:[49]

$$\vec{P}_{SSHG}(2\omega) = \vec{P}^{(2)}(2\omega) + \vec{P}^{(3)}(2\omega) = \varepsilon_0 \vec{\vec{\chi}}^{(2)}(2\omega, \omega, \omega)\vec{E}(\omega)\vec{E}(\omega) + \varepsilon_0 \vec{\vec{\chi}}^{(3)}(2\omega, \omega, \omega, 0)\vec{E}(\omega)\vec{E}(\omega)\vec{\Phi}(0) \quad (1)$$

where $\vec{\vec{\chi}}^{(3)}$ is the third-order nonlinear electric susceptibility tensor and $\vec{E}(\omega)$ is the electric field oscillating at the probe frequency, ω.

Because of this static field, the SSHG signal can also originate from partially oriented MG dyes located in the bulk region close to the interface. If the increased SSHG intensity observed upon small additions of SDS were due to this effect, the TR-SSHG profiles should mostly reflect the excited-state dynamics of MG in bulk water. In such case, the profiles would be totally different than those measured here. Indeed, at 10^{-5} M, MG is only present as a monomer in bulk water and its excited-state lifetime amounts to about 600 fs.[37] The absence of the fast TR-SSHG component at small SDS concentration indicates that the SSHG signal is essentially of a dipolar nature and due to MG aggregates and that the contribution from the third-order nonlinear polarization is not significant here.

At 4 mM and higher SDS concentrations, the stationary SSHG intensity decreases and the TR-SSHG dynamics accelerates. In consideration that a SDS monolayer at the air/water interface is achieved at approximately 6 mM,[50] these observed changes of the SSHG signal occur when the interface is almost entirely covered by SDS. Indeed, Eisenthal and coworkers showed that, in the presence of a surface-active dye, the

dx.doi.org/10.1021/la402191p | Langmuir 2013, 29, 14865−14872

saturation of the interfacial SDS concentration occurs substantially below 6 mM.[51] Richmond and co-workers have measured a decrease of the SSFG intensity associated with several SDS vibrations at the air/water interface upon increasing SDS concentration above approximately 2 mM and tentatively ascribed it to an increase of the alkyl chain disorder brought about by micelle formation.[50] It is difficult to account for the effects observed here with MG in terms of chain disorder. We rather propose that these effects are due to the superior affinity of SDS for the interface compared to MG. At small SDS concentrations, the surface coverage is low and the negative charge of the interface favors adsorption and, hence, aggregation of MG. Increasing SDS concentration augments the coverage of the interface and, despite the electrostatic interaction, inhibits adsorption of MG. This leads to a decrease of the adsorbed MG population, hence, the stationary SSHG intensity, and to a smaller population of aggregates, thus to a faster recovery of the TR-SSHG profile. A decrease of SSHG signal intensity due to competitive adsorption was already reported for air−liquid and liquid−solid interfaces.[52,53] As the interface is no longer accessible to MG once fully covered by SDS, electrostatic interaction with the SDS should lead to the accumulation of MG in the subinterfacial region. The decrease of the SSHG intensity indicates that these MG molecules are either randomly oriented or that their orientation does not lead to a significant SSHG signal. Because the resonant enhancement is due to a transition with the dipole oriented along the main molecular axis of MG, a SSHG signal is only obtained if the average angle between the main molecular axis and the interfacial plane differs from zero.

Similar stationary SSHG and TR-SSHG measurements have been performed with the cationic surfactant CTAB. At 0.1 mM CTAB, the SSHG intensity decreases to a level close to the limit of detection. This result can be very well-explained in terms of the electrostatic repulsion between the positively charged CTAB surfactant and the cationic MG molecules. Since CTAB exhibits even bigger interfacial affinity than SDS,[54,55] its addition results in a positive charging of the interface and to the repulsion of the cationic MG dyes from the interface.

The above experiments were repeated with the EB dianion (Chart 1) instead of MG. The stationary SSHG spectrum of EB at the water/dodecane interface peaks around 425 nm (Figure S5 of the Supporting Information) and most probably originates from a $S_2 \leftarrow S_0$ two-photon resonance. Upon addition of CTAB, the stationary SSHG intensity increases up to a surfactant concentration of approximately 0.1 mM and then decreases down to reach a value close to that without CTAB at concentrations exceeding the CMC of 0.9 mM (Figure 7 inset).[56] Upon excitation of EB at 515 nm, the TR-SSHG intensity decreases, due to a depletion of the ground-state population and recovers its original value after about 60 ps (Figure 7). Upon addition of CTAB, the ground-state recovery accelerates up to 0.1 mM and slows down at higher concentrations. Above 1 mM, the dynamics becomes even slower than without surfactant. Previous TR-SSHG studies with EB at the alkane/water interface revealed a substantial acceleration of the ground-state recovery upon increasing the bulk concentration of EB.[57] This effect was ascribed to the increasing contribution of EB aggregates, known to have a short excited-state lifetime,[58] to the SSHG signal. Therefore, the acceleration of the TR-SSHG dynamics upon addition of 0.1 mM CTAB can be ascribed to a higher interfacial population of EB, whereas the subsequent slowing down upon further addition of CTAB is due to a lower population of adsorbed EB molecules. This behavior is very similar to that observed with MG upon addition of SDS and can be interpreted likewise, i.e., an enhancement of interfacial dye population at small surfactant concentration favored by electrostatic interactions, followed by a depletion of the dye molecules from the interface due to its coverage by the surfactant.

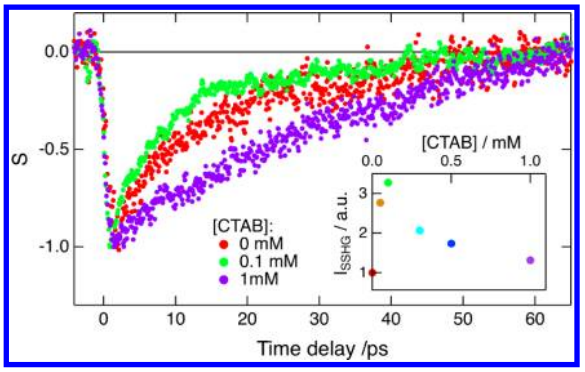

Figure 7. TR-SSHG profiles measured at 400 nm with EB (10^{-4} M) and different concentrations of CTAB at the dodecane/water interface. Inset: dependence of the stationary SSHG intensity at the band maximum on the CTAB concentration.

The surfactant concentration at which the strongest effect is observed on both the TR-SSHG profile and the SSHG intensity is smaller by about 1 order of magnitude with CTAB than with SDS (insets of Figures 6 and 7). This difference can be accounted for by the higher adsorption efficiency of CTAB compared to SDS, as reflected by the pC_{20} values, which amount to 3.4 and 2.4 for CTAB and SDS at the air/water interfaces.[59,60] This pC_{20} parameter is the negative logarithm of the surfactant concentration needed to reduce the surface tension by 20 mN/m. This concentration has been shown to be close to that required to saturate the interface.[61]

Finally, addition of SDS had the same effect on the SSHG signal of EB than that of CTAB with MG, as expected. Indeed, the SSHG signal intensity decreases dramatically, even at very small SDS concentrations, and above 0.1 mM SDS, no SSHG signal can be detected. Here again, the large interfacial affinity of SDS leads to a negative charging of the interface and the dianionic EB molecules are thus repelled.

■ CONCLUSIONS

This investigation shows univocally that the interfacial population of charged dyes can be controlled by adding small amounts of ionic surfactants. Adsorption of the dye is enhanced when using oppositely charged surfactants, whereas depletion of the dye occurs when adding a surfactant with the same charge. However, independently of the relative charges of dye and surfactant, a large interfacial coverage by the surfactant substantially decreases the dye population, due to the smaller affinity of the latter for the interface. Such effects are only expected with dyes like those used here, which have a good solubility in water and are not highly surface active.

This investigation gives a firm ground to our previous explanation for the effect of salts on the interfacial dynamics of MG. The presence of a salting-in anion like SCN^- in the aqueous phase has the same effect as that of SDS, which, being a surfactant, has a strong interfacial affinity. We can thus conclude that the enhanced aggregation of MG upon addition of SCN^- indeed originates from the affinity of this anion for the

dx.doi.org/10.1021/la402191p | Langmuir 2013, 29, 14865−14872

interface, and thus to its higher concentration in the interfacial region relative to the bulk solution. Therefore, the amount of aggregation of MG, measured by TR-SSHG, is a powerful probe of the relative interfacial affinity of anions. On the other hand, we found that the guanidinium cation has not the same effect as the cationic surfactant CTAB, indicating that this cation is rather depleted from the interface, as also concluded from previous surface tension measurements and molecular dynamics simulations.[17,47]

Most of the TR-SSHG experiments reported so far have been done at a single probe wavelength. We showed here with MG that access not only to the SSHG spectrum but also to the TR-SSHG profiles recorded at several wavelengths greatly facilitates data interpretation. Efforts toward the measurements of entire TR-SSHG spectra are needed to bring these interface-selective techniques at a level close to that of the methods available for the investigation of bulk solutions.

■ ASSOCIATED CONTENT

Supporting Information

Stationary SSHG spectra of MG and EB with and without salt, TR-SSHG profiles measured with MG with NaSCN and with SDS. This material is available free of charge via the Internet at http://pubs.acs.org.

■ AUTHOR INFORMATION

Corresponding Author

*E-mail: eric.vauthey@unige.ch.

Present Address

[†]Institute of Experimental Physics, Faculty of Physics, University of Warsaw, ul. Hoża 69, Warsaw, Poland.

Notes

The authors declare no competing financial interest.

■ ACKNOWLEDGMENTS

We wish to thank Mr. Dominique Lovy for his inestimable help in the development of the surface-second harmonic generation experiments. The contribution of Ms. Sabine Richert to the construction of the new time-resolved surface-second harmonic generation setup is also acknowledged. This work was supported by the Swiss National Science Foundation through Grants 200020-134471 and 200020-147098 and the NCCR MUST.

■ REFERENCES

(1) Watarai, H.; Teramae, N.; Sawada, T. *Interfacial Nanochemistry*; Kluwer Academic: New York, 2005.

(2) Volkov, A. G. E. *Liquid Interfaces in Chemical, Biological, and Pharmaceutical Applications*; Marcel Dekker: New York, 2001.

(3) Adamson, A. W. *Physical Chemistry of Surfaces*, 4th ed.; Wiley: New York, 1982.

(4) Fermin, D. J.; Duong, H. D.; Ding, Z.; Brevet, P. F.; Girault, H. H. Solar energy conversion using dye-sensitised liquidlliquid interfaces. *Electrochem. Commun.* **1999**, *1*, 29−32.

(5) Steel, W. H.; Walker, R. A. Measuring Dipolar Width across Liquid-Liquid Interfaces with 'Molecular Rulers'. *Nature* **2003**, *424*, 296−299.

(6) Heinz, T. F.; Chen, C. K.; Ricard, D.; Shen, Y. R. Spectroscopy of molecular monolayers by resonant second-harmonic generation. *Phys. Rev. Lett.* **1982**, *48*, 478−481.

(7) Hicks, J. M.; Kemnitz, K.; Eisenthal, K. B.; Heinz, T. F. Studies of liquid surfaces by second harmonic generation. *J. Phys. Chem.* **1986**, *90*, 560−562.

(8) Richert, S.; Fedoseeva, M.; Vauthey, E. Ultrafast photoinduced dynamics at air/liquid and liquid/liquid interfaces. *J. Phys. Chem. Lett.* **2012**, *3*, 1635−1642.

(9) Richmond, G. L. Molecular bonding and interactions at aqueous surfaces as probed by vibrational sum frequency spectroscopy. *Chem. Rev.* **2002**, *102*, 2693−724.

(10) Sekiguchi, K.; Yamaguchi, S.; Tahara, T. Femtosecond time-resolved electronic sum-frequency generation spectroscopy: A new method to investigate ultrafast dynamics at liquid interfaces. *J. Chem. Phys.* **2008**, *128*, 114715.

(11) Boyd, R. W., *Nonlinear Optics*, 3rd ed.; Academic Press: Orlando, 2008.

(12) Petersen, P. B.; Saykally, R. J. On the nature of ions at the liquid water surface. *Annu. Rev. Phys. Chem.* **2006**, *57*, 333−364.

(13) Ball, P. Water as an active constituent in cell biology. *Chem. Rev.* **2007**, *108*, 74−108.

(14) Lo Nostro, P.; Ninham, B. W. Hofmeister phenomena: An update on ion specificity in biology. *Chem. Rev.* **2012**, *112*, 2286−2322.

(15) Flores, S. C.; Kherb, J.; Konelick, N.; Chen, X.; Cremer, P. S. The effects of Hofmeister cations at negatively charged hydrophilic surfaces. *J. Phys. Chem. C* **2012**, *116*, 5730−5734.

(16) Abel, B. Hydrated interfacial ions and electrons. *Annu. Rev. Phys. Chem.* **2013**, *64*, 533−52.

(17) Pegram, L. M.; Record, M. T. Hofmeister salt effects on surface tension arise from partitioning of anions and cations between bulk water and the air−water interface. *J. Phys. Chem. B* **2007**, *111*, 5411−7.

(18) Lyklema, J. Simple Hofmeister series. *Chem. Phys. Lett.* **2009**, *467*, 217−22.

(19) Parsons, D. F.; Bostrom, M.; Nostro, P. L.; Ninham, B. W. Hofmeister effects: Interplay of hydration, nonelectrostatic potentials, and ion size. *Phys. Chem. Chem. Phys.* **2011**, *13*, 12352−67.

(20) Fedoseeva, M.; Fita, P.; Punzi, A.; Vauthey, E. Salt Effect on the Formation of Dye Aggregates at Liquid/Liquid Interfaces Studied by Time-Resolved Surface Second Harmonic Generation. *J. Phys. Chem. C* **2010**, *114*, 13774−13781.

(21) Becraft, K. A.; Moore, F. G.; Richmond, G. L. In-situ spectroscopic investigations of surfactant adsorption and water structure at the CaF2/aqueous solution interface. *Phys. Chem. Chem. Phys.* **2004**, *6*, 1880−9.

(22) Liu, D.; Ma, G.; Levering, L. M.; Allen, H. C. Vibrational spectroscopy of aqueous sodium halide solutions and air−liquid interfaces: Observation of increased interfacial depth. *J. Phys. Chem. B* **2004**, *108*, 2252−60.

(23) Raymond, E. A.; Richmond, G. L. Probing the molecular structure and bonding of the surface of aqueous salt solutions. *J. Phys. Chem. B* **2004**, *108*, 5051−5059.

(24) Petersen, P. B.; Saykally, R. J. Confirmation of enhanced anion concentration at the liquid water surface. *Chem. Phys. Lett.* **2004**, *397*, 51−55.

(25) Petersen, P. B.; Saykally, R. J. Probing the interfacial structure of aqueous electrolytes with femtosecond second harmonic generation spectroscopy. *J. Phys. Chem. B* **2006**, *110*, 14060−14073.

(26) Koelsch, P.; Motschmann, H. Varying the counterions at a charged interface. *Langmuir* **2005**, *21*, 3436−3442.

(27) Santos, C. S.; Rivera-Rubero, S.; Dibrov, S.; Baldelli, S. Ions at the surface of a room-temperature ionic liquid. *J. Phys. Chem. C* **2007**, *111*, 7682−91.

(28) Levering, L. M.; Sierra-Hernandez, M. R.; Allen, H. C. Observation of hydronium ions at the air-aqueous acid interface: Vibrational spectroscopic studies of aqueous HCl, HBr, and HI. *J. Phys. Chem. C* **2007**, *111*, 8814−8826.

(29) Onorato, R. M.; Otten, D. E.; Saykally, R. J. Adsorption of thiocyanate ions to the dodecanol/water interface characterized by UV second harmonic generation. *Proc. Natl. Acad. Sci. U.S.A.* **2009**, *106*, 15176−80.

(30) Xu, M.; Tang, C. Y.; Jubb, A. M.; Chen, X.; Allen, H. C. Nitrate anions and ion pairing at the air−aqueous interface. *J. Phys. Chem. C* **2009**, *113*, 2082−2087.

(31) Viswanath, P.; Aroti, A.; Motschmann, H.; Leontidis, E. Vibrational sum frequency generation spectroscopic investigation of the interaction of thiocyanate ions with zwitterionic phospholipid monolayers at the air/water interface. *J. Phys. Chem. B* **2009**, *113*, 14816−23.
(32) Hua, W.; Chen, X.; Allen, H. C. Phase-sensitive sum frequency revealing accommodation of bicarbonate ions, and charge separation of sodium and carbonate ions within the air/water interface. *J. Phys. Chem. A* **2011**, *115*, 6233−8.
(33) Shamay, E. S.; Richmond, G. L. Ionic disruption of the liquid-liquid interface. *J. Phys. Chem. C* **2010**, *114*, 12590−12597.
(34) Jungwirth, P.; Tobias, D. J. Specific ion effects at the air/water interface. *Chem. Rev.* **2006**, *106*, 1259−1281.
(35) Baer, M. D.; Mundy, C. J. Toward an understanding of the specific ion effect using density functional theory. *J. Phys. Chem. Lett.* **2011**, *2*, 1088−1093.
(36) Bauer, B. A.; Ou, S.; Patel, S. Role of spatial ionic distribution on the energetics of hydrophobic assembly and properties of the water/hydrophobe interface. *Phys. Chem. Chem. Phys.* **2012**, *14*, 1892−1906.
(37) Fita, P.; Punzi, A.; Vauthey, E. Local viscosity of binary water +glycerol mixtures at liquid/liquid interfaces probed by time-resolved surface second harmonic generation. *J. Phys. Chem. C* **2009**, *113*, 20705−12.
(38) Nguyen, K. T.; Shang, X.; Eisenthal, K. B. Molecular rotation at negatively charged surfactant/aqueous interfaces. *J. Phys. Chem. B* **2006**, *110*, 19788−92.
(39) Beaman, D. K.; Robertson, E. J.; Richmond, G. L. From head to tail: Structure, solvation, and hydrogen bonding of carboxylate surfactants at the organic-water interface. *J. Phys Chem. C* **2011**, *115*, 12508−12516.
(40) Punzi, A.; Martin-Gassin, G.; Grilj, J.; Vauthey, E. Effect of salt on the excited-state dynamics of malachite green in bulk aqueous solutions and at air/water interfaces: A femtosecond transient absorption and surface second harmonic generation study. *J. Phys. Chem. C* **2009**, *113*, 11822−11829.
(41) Fedoseeva, M.; Richert, S.; Vauthey, E. Excited-state dynamics of organic dyes at liquid-liquid interfaces. *Langmuir* **2012**, *28*, 11291−11301.
(42) Shen, Y. R. Surface contribution versus bulk contribution in surface nonlinear optical spectroscopy. *Appl. Phys. B: Lasers Opt.* **1999**, *68*, 295−300.
(43) Lang, B.; Angulo, G.; Vauthey, E. Ultrafast solvation dynamics of coumarin 153 in imidazolium based ionic liquids. *J. Phys. Chem. A* **2006**, *110*, 7028.
(44) Sen, P.; Yamaguchi, S.; Tahara, T. Ultrafast dynamics of malachite green at the air-water interface studied by femtosecond time-resolved electronic sum frequency generation (TR-ESFG): an indicator for local viscosity. *Faraday Discuss.* **2010**, *145*, 411−28.
(45) Shi, X.; Borguet, E.; Tarnovsky, A. N.; Eisenthal, K. B. Ultrafast dynamics and structure at aqueous interfaces by second harmonic generation. *Chem. Phys.* **1996**, *205*, 167−178.
(46) Smith, J. S.; Scholtz, J. M. Guanidine hydrochloride unfolding of peptide helices: Separation of denaturant and salt effects. *Biochemistry* **1996**, *35*, 7292−7297.
(47) Wernersson, E.; Heyda, J.; Vazdar, M.; Lund, M.; Mason, P. E.; Jungwirth, P. Orientational dependence of the affinity of guanidinium ions to the water surface. *J. Phys. Chem. B* **2011**, *115*, 12521−6.
(48) Gragson, D. E.; McCarty, B. M.; Richmond, G. L. Surfactant/water interactions at the air/water interface probed by vibrational sum frequency generation. *J. Phys. Chem.* **1996**, *100*, 14272−5.
(49) Zhao, X.; Ong, S.; Eisenthal, K. B. Polarization of water molecules at a charged interface. Second harmonic studies of charged monolayers at the air/water interface. *Chem. Phys. Lett.* **1993**, *202*, 513−520.
(50) Gragson, D. E.; McCarty, B. M.; Richmond, G. L. Ordering of interfacial water molecules at the charged air/water interface observed by vibrational sum frequency generation. *J. Am. Chem. Soc.* **1997**, *119*, 6144−6152.
(51) Benderskii, A. V.; Eisenthal, K. B. Dynamical timescales of aqueous solvation at negatively charged lipid/water interfaces. *J. Phys. Chem. A* **2002**, *106*, 7482−7490.
(52) Wang, H.; Troxler, T.; Yeh, A.-G.; Dai, H.-L. In Situ, nonlinear optical probe of surfactant adsorption on the surface of microparticles in colloids. *Langmuir* **2000**, *16*, 2475−2481.
(53) Sahu, K.; Eisenthal, K. B.; McNeill, V. F. Competitive adsorption at the air−water interface: A second harmonic generation study. *J. Phys. Chem. C* **2011**, *115*, 9701−9705.
(54) Edler, K. J.; Wasbrough, M. J.; Holdaway, J. A.; O'Driscoll, B. M. Self-assembled films formed at the air-water interface from CTAB/SDS mixtures with water-soluble polymers. *Langmuir* **2009**, *25*, 4047−4055.
(55) Tah, B.; Pal, P.; Mahato, M.; Talapatra, G. B. Aggregation behavior of SDS/CTAB catanionic surfactant mixture in aqueous solution and at the air/water interface. *J. Phys. Chem. B* **2011**, *115*, 8493−9.
(56) Chattopadhyay, A.; London, E. Fluorimetric determination of critical micelle concentration avoiding interference from detergent charge. *Anal. Biochem.* **1984**, *139*, 408−412.
(57) Fita, P.; Fedoseeva, M.; Vauthey, E. Hydrogen-bond-assisted excited-state deactivation at liquid/water interfaces. *Langmuir* **2011**, *27*, 4645−4652.
(58) Valdes-Aguilera, O.; Neckers, D. C. Aggregation phenomena in xanthene dyes. *Acc. Chem. Res.* **1989**, *22*, 171−177.
(59) Chakraborty, T.; Ghosh, S.; Moulik, S. P. Micellization and related behavior of binary and ternary surfactant mixtures in aqueous medium: Cetyl Pyridinium Chloride (CPC), Cetyl Trimethyl Ammonium Bromide (CTAB), and Polyoxyethylene (10) Cetyl Ether (Brij-56) derived system. *J. Phys. Chem. B* **2005**, *109*, 14813−23.
(60) Elworthy, P. H.; Mysels, K. J. The surface tension of sodium dodecylsulfate solutions and the phase separation model of micelle formation. *J. Colloid Interface Sci.* **1966**, *21*, 331−347.
(61) Rosen, M. J. *Surfactants and Interfacial Phenomena*; Wiley: New York, 1978.